

S-pairing in neutron matter

I. Correlated Basis Function Theory

Adelchi Fabrocini*

*Dipartimento di Fisica "Enrico Fermi", Università di Pisa and
INFN, Sezione di Pisa, I-56100 Pisa, Italy*

Stefano Fantoni†

*International School for Advanced Studies, SISSA and
INFN DEMOCRITOS National Simulation Center, I-34014 Trieste, Italy*

Alexey Yu. Illarionov‡

*International School for Advanced Studies, SISSA, I-34014 Trieste, Italy and
INFN, Sezione di Pisa, I-56100 Pisa, Italy*

Kevin E. Schmidt§

*Department of Physics and Astronomy, Arizona State University, Tempe, AZ, 85287 and
International School for Advanced Studies, SISSA, I-34014 Trieste, Italy
(Dated: March 9, 2022)*

S-wave pairing in neutron matter is studied within an extension of correlated basis function (CBF) theory to include the strong, short range spatial correlations due to realistic nuclear forces and the pairing correlations of the Bardeen, Cooper and Schrieffer (BCS) approach. The correlation operator contains central as well as tensor components. The correlated BCS scheme of Ref. [1], developed for simple scalar correlations, is generalized to this more realistic case. The energy of the correlated pair condensed phase of neutron matter is evaluated at the two-body order of the cluster expansion, but considering the one-body density and the corresponding energy vertex corrections at the first order of the Power Series expansion. Based on these approximations, we have derived a system of Euler equations for the correlation factors and for the BCS amplitudes, resulting in correlated non linear gap equations, formally close to the standard BCS ones. These equations have been solved for the momentum independent part of several realistic potentials (Reid, Argonne v_{14} and Argonne $v_{8'}$) to stress the role of the tensor correlations and of the many-body effects. Simple Jastrow correlations and/or the lack of the density corrections enhance the gap with respect to uncorrelated BCS, whereas it is reduced according to the strength of the tensor interaction and following the inclusion of many-body contributions.

PACS numbers: 02.70.Ss, 2.70.Uu, 03.75.Hh, 03.75.Kk, 03.75.Mn, 05.10.Ln, 05.30.Fk, 05.70.Fh, 21.30.-x, 21.60.-n, 21.60.Gx, 21.60.Ka, 21.65.+f, 26.60.+c, 67.40.Db

Keywords: nuclear forces, nuclear matter, nuclear cluster models, nuclear pairing, superfluidity

I. INTRODUCTION

Superfluidity in neutron matter has been a fascinating topic in many-body physics and astrophysics ever since Migdal [2] proposed the possibility of superfluid matter in neutron stars. In the inner crust of the star, 1S_0 pairing in the low density neutron gas permeating the lattice of neutron rich nuclei may occur and peak at densities much lower than the empirical nuclear matter saturation density, $\rho_0 = 0.16 \text{ fm}^{-3}$. A similar pairing may take place for the low concentration proton component in the highly asymmetrical nuclear matter in the star's interior. At higher interior densities, neutrons may also pair in the anisotropic 3P_2 - 3F_2 partial wave. A realistic evaluation of the density regimes where superfluidity takes place and of the strength of the connected energy gaps is needed for a quantitative understanding of important features of neutron stars, such as the cooling rate[3, 4] and the post-glitch relaxation times [5, 6].

*Electronic address: Adelchi.Fabrocini@df.unipi.it

†Electronic address: fantoni@sissa.it

‡Electronic address: illario@sissa.it

§Electronic address: Kevin.Schmidt@asu.edu

The qualitative aspects of superfluidity were shown to be describable in nuclei [7] and in infinite systems of interacting fermions [8] by the extension of the theory of superconductivity of Bardeen, Cooper and Schrieffer [9] (BCS). In terms of the nucleon–nucleon (NN) interaction, it is the long range attraction of the 1S_0 NN potential that dominates in the inner crust density regime, allowing for S -wave pairing. The gap closes with rising density since the short range repulsion is more and more effective. Proton superfluidity (or superconductivity) has a similar origin in the interior, while higher density 3P_2 – 3F_2 neutron pairing is traced back to non central, tensor and spin–orbit, components. In BCS theory Cooper–like pairs allow for superfluidity even in presence of the short range repulsion of modern potentials.

On the other hand, the strong nuclear interaction induces short range correlations in the wave function, which also largely screen the repulsion and introduce many–body contributions. These two features have competing effects, since the former is expected to increase the gap, whereas the latter may diminish it. Modern many–body theories, such as the method of correlated basis functions [10] (CBF), the Bethe–Brueckner–Goldstone expansion [11] (BBG), the self–consistent Green’s functions theory [12] (SCGF), and lately quantum Monte Carlo [13] (QMC), can, with efficiency and accuracy, deal with short range correlations in normal phase nucleonic matter. It can be reasonably expected that these methods also may be able to provide a similarly realistic description of the superfluid phase, especially when modern NN potentials are used.

Within CBF the short range correlations are introduced by acting with a many–body correlation operator on a set of model functions, so defining a correlated basis to be used in a perturbative expansion where the highly non perturbative short range correlation effects are already embedded in the basis. The zeroth order of the correlated perturbative expansion corresponds to a variational approach, since the correlation operator (and the ground-state model wave function) can be derived applying the Ritz variational principle. The variational level may already give reliable results if the correlation operator is chosen in an appropriate way. Because realistic NN potentials have important spin– and isospin–dependent components, both central and non central (e.g the tensor potential, mainly originating from one–pion exchange), a good variational choice for the pair correlation $\hat{f}(ij)$ must include at least six components,

$$\hat{f}_6(ij) = \sum_{p=1,6} f^{(p)}(r_{ij}) \hat{O}^{(p)}(ij), \quad (1)$$

where $\hat{O}^{(p=1,2,3)}(ij) = 1$, $\sigma(i) \cdot \sigma(j)$, $\hat{S}(ij) = (3\hat{r}_\alpha(ij)\hat{r}_\beta(ij) - \delta_{\alpha\beta})\sigma_\alpha(i)\sigma_\beta(j)$, and $\hat{O}^{(p'=p+3)}(ij) = \hat{O}^{(p)}(ij) \otimes \tau(i) \cdot \tau(j)$. The greek indices denote the Cartesian components. This choice of the operatorial dependence of the correlation is consistent with the use of the non central and momentum independent v_6 potentials of the form,

$$\hat{v}_6(ij) = \sum_{p=1,6} v^{(p)}(r_{ij}) \hat{O}^{(p)}(ij). \quad (2)$$

However, $\hat{f}_6(ij)$ is in general a very good variational choice *for all* the realistic potentials. The introduction of such structures directly in the correlation operators allows the variational approach to describe microscopically the structure of nuclear matter [14] and finite nuclei [15] with a good accuracy.

In this paper we are only dealing with pure neutron matter (PNM), therefore $\tau(i) \cdot \tau(j) \equiv 1$ and the 6–operator algebra underlying $\hat{v}_6(ij)$ and $\hat{f}_6(ij)$ reduces to the first 3 components $p = 1, 2, 3$, where $f_{\text{PNM}}^{(p)} = f^{(p)} + f^{(p+3)}$ and $v_{\text{PNM}}^{(p)} = v^{(p)} + v^{(p+3)}$.

Since the operators in (1) do not commute, the many–body correlation operator, $\hat{F}_6(1, 2, \dots, N)$, is given by the symmetrized product,

$$\hat{F}_6(1, 2, \dots, N) = \mathcal{S} \left[\prod_{i < j = 1, N} \hat{f}_6(ij) \right]. \quad (3)$$

In CBF theory such operators are kept fixed for all the intermediate states. The correlated CBF intermediate states are obtained by acting with $\hat{F}_6(1, 2, \dots, N)$ on the corresponding uncorrelated Slater determinant.

An alternative approach, hereafter denoted as CBF-J, consists in starting with a simpler Jastrow correlation [10], depending only on the interparticle distance,

$$F_J(1, 2, \dots, N) = \prod_{i < j = 1, N} f_J(r_{ij}), \quad (4)$$

and introducing the spin/isospin dependence via a Jastrow–correlated perturbative expansion [16]. This choice may not be very efficient since the whole spin-isospin dependence must be perturbatively included. However, the terms

of the CBF-J expansion have a much simpler structure than those of the CBF expansion, based on spin dependent correlation operators, and can be computed by Fermi hypernetted chain (FHNC) resummation [1]. A possible drawback of the CBF-J perturbative expansion is the complexity of going beyond the second order perturbation level which may be insufficient in the Jastrow-like CBF theory.

Variational CBF theory has been applied to the S -wave nucleonic superfluid in Ref. [17] using central potentials and correlations, without tensor components,

$$\hat{v}_4(ij) = \sum_{S,T=0,1} v^{(ST)}(r_{ij}) \hat{P}^{(ST)}(ij), \quad (5)$$

$$\hat{f}_4(ij) = \sum_{S,T=0,1} f^{(ST)}(r_{ij}) \hat{P}^{(ST)}(ij), \quad (6)$$

where $\hat{P}^{(ST)}(ij)$ are projectors onto the two-body subspace of total spin-isospin ST . The N -body correlation operator is then given by:

$$\hat{F}_4(1, 2, \dots, N) = \mathcal{S} \left[\prod_{i < j = 1, N} \hat{f}_4(ij) \right]. \quad (7)$$

Lowest order cluster expansion was used to derive a correlated gap equation with the \hat{v}_4 version of the Reid soft core NN interaction [18, 19]. This correlated theory was developed within the independent Cooper pairs approximation and does not consider the dependence of the correlation on the BCS amplitudes. The approach takes essentially into account the screening of the core repulsion due to the repulsive part of the correlation, and leads to a larger gap than BCS. Chen et al. [16] studied S -pairing with the Reid v_6 potential, including the interaction tensor components, using the independent Cooper pairs approximation. They considered a simple Jastrow correlation rather than the correlation operator \hat{F}_6 of Eq. 1, but computed the variational energy at a higher level of the cluster expansion through FHNC theory [20]. A reduction of the BCS gap of about 30% was found, attributable, however, to a rather poor choice of the Jastrow factor. The authors of Ref. [16] also computed the second order perturbative CBF correction to the pairing matrix element on top of the Jastrow estimate. This approach, which should take into account *medium polarization*, led to a dramatic reduction of the gap by $\sim 80\%$, much larger than all the other estimates of the polarization effects, and inconsistent with X-ray observations [21]. In spite of the fact that the matrix elements of CBF perturbation theory are easier to compute in a Jastrow correlated basis, its convergence for large non-central potentials in such a basis is still to be assessed.

The independent Cooper pairs approximation was overcome in ref. [1], hereafter denoted as I, with a Jastrow fully correlated BCS theory. In this work we begin to extend the work of I to the case of correlations having spin-isospin dependent, with both central and tensor components (f_6 model).

The use of a f_6 correlation does not allow for a complete sum of the FHNC diagrams, very much the same as for the case of normal phase. Similarly to that case the massive resummations of diagrams can be performed using the single operator chain (SOC) approximation of Ref. [19]. In this paper we limit our attention to study pure neutron matter at the two-body level plus vertex corrections of the cluster expansion of $\langle \hat{H} - \mu \hat{N} \rangle$, where μ is the chemical potential determined by fixing the correct mean value of the particle number operator (or the density, for infinite systems) $\langle \hat{N} \rangle = \sum_m \langle a_m^\dagger a_m \rangle$.

The one-body density $\rho = \langle \hat{N} \rangle / \Omega$, and consequently the vertex corrections in $\langle \hat{H} \rangle$, will be here computed at the first order of the Power Series expansion [20]. This approximation guarantees in the normal phase the correct density normalization, order by order, and introduces a first flavor of many-body effects. The expectation value $\langle \hat{H} \rangle$ will be computed at the second order of the cluster expansion, which provides a sufficiently good description of the short-range correlations.

Minimization of $\langle \hat{H} - \mu \hat{N} \rangle_2$ with respect to the correlation functions f_6 and to the BCS amplitudes leads to a coupled set of Euler and gap equations, which we denote as correlated BCS equation. The solution of such equation is a preliminary, very important step towards a full calculation, which will include higher order effects in the evaluation of both $\langle \hat{N} \rangle$ and $\langle \hat{H} \rangle$ and second order perturbative corrections following orthogonal CBF theory of ref. [22]. A second approach consists in using the Auxiliary Field Diffusion Monte Carlo (AFDMC) method to calculate the gap energy of a finite number of neutrons in the superfluid phase. Such a method has been used to simulate up to 114 neutrons in a periodical box to evaluate the equation of state at zero temperature in neutron matter in the normal phase [23]. The extension to superfluid phases can be done using the method developed in the recent work [24] in the study of low density Fermi gas in the regime of large scattering length interaction. AFDMC simulations of this type crucially depend upon the choice of a guiding function to fix the nodes and the phases of the wave

function. Therefore, the BCS amplitudes resulting from solving the correlated BCS equation are a fundamental input to the AFDMC simulations. Preliminary results of that simulations performed with 14 neutrons have already been published [25]. Besides the derivation of the correlated BCS equation and its solution for several potentials of the v_6 type (like the truncated versions of the Reid [18], Argonne v_{14} and Argonne v_8 [26] potentials) we have evaluated the gap energy with and without vertex corrections. The latter to compare with BBG [11] and SCGF [12], the former to estimate the effect of the three-body terms of which the vertex corrections are the main part.

The plan of the paper is as follows: in Section 2 the correlated BCS theory for a f_6 correlation is presented; Section 3 contains the Euler and correlated gap equations; numerical results and details on the solution of the equations are given in Section 4; Section 5 will briefly discuss our results and give conclusions and perspectives

II. CORRELATED BCS THEORY

A correlated wave function for the neutron matter superfluid phase is constructed as

$$|\Psi_s\rangle = \hat{F} |\text{BCS}\rangle, \quad (8)$$

where the model BCS-state vector is

$$|\text{BCS}\rangle = \prod_{\mathbf{k}} (u_{\mathbf{k}} + v_{\mathbf{k}} a_{\mathbf{k}\uparrow}^\dagger a_{-\mathbf{k}\downarrow}^\dagger) |0\rangle. \quad (9)$$

$u_{\mathbf{k}}$ and $v_{\mathbf{k}}$ are the real variational BCS amplitudes, satisfying the relation $u_{\mathbf{k}}^2 + v_{\mathbf{k}}^2 = 1$, $|0\rangle$ is the vacuum state and a_m^\dagger is the fermion creation operator in the single-particle state $|m = \mathbf{k}, \sigma\rangle$ whose wave function is

$$\langle x \equiv \mathbf{r}, s | a_m^\dagger | 0 \rangle = \phi_{m \equiv \mathbf{k}, \sigma}(x \equiv \mathbf{r}, s) = \frac{1}{\sqrt{\Omega}} \eta_\sigma(s) \exp(i\mathbf{k} \cdot \mathbf{r}). \quad (10)$$

Ω is the normalization volume and $\eta_{\sigma=\uparrow, \downarrow}(s)$ is the spin wave function with spin projection σ . The second-quantized correlation operator \hat{F} is written in terms of the N -particle correlation operators, \hat{F}_N , as

$$\hat{F} = \sum_{N, m_N} \hat{F}_N |\Phi_N^{m_N}\rangle \langle \Phi_N^{m_N}|, \quad (11)$$

where m_N specifies a set of N single-particle states with $N = 0, 2, 4, \dots$. In coordinate representation and for a f_6 -type correlation we have:

$$\langle x_1, x_2, \dots, x_N | \hat{F}_N |\Phi_N^{m_N}\rangle = \hat{F}_6(1, 2, \dots, N) \{ \phi_{m_1}(x_1) \phi_{m_2}(x_2) \dots \phi_{m_N}(x_N) \}_A. \quad (12)$$

The suffix A stands for an antisymmetrized product of single-particle wave functions and $\hat{F}_6(1, 2, \dots, N)$ is the f_6 N -particle correlation operator (3).

In I the cluster expansions of the two-body distribution function, $g(r_{12})$,

$$g(r_{12}) = \frac{1}{\mathcal{N} \rho^2} \sum_{\sigma_1, \sigma_2} \langle \Psi_s | \Psi_{\sigma_1}^\dagger(\mathbf{r}_1) \Psi_{\sigma_1}(\mathbf{r}_1) \Psi_{\sigma_2}^\dagger(\mathbf{r}_2) \Psi_{\sigma_2}(\mathbf{r}_2) | \Psi_s \rangle, \quad (13)$$

and of the one-body density matrix, $n(r_{11'})$,

$$n(r_{11'}) = \frac{1}{\mathcal{N}} \sum_{\sigma_1, \sigma_{1'}} \langle \Psi_s | \Psi_{\sigma_1}^\dagger(\mathbf{r}_1) \Psi_{\sigma_{1'}}(\mathbf{r}_{1'}) | \Psi_s \rangle, \quad (14)$$

in the Jastrow correlated case were studied. In the above equations, \mathcal{N} are normalization constants, $\Psi_\sigma(\mathbf{r})$ and $\Psi_\sigma^\dagger(\mathbf{r})$ are the destruction and creation field operators.

In I it was proved that $g(r_{12})$ and $n(r_{11'})$ are given by the sum of all the linked cluster diagrams, constructed by the dynamical correlation lines ($h_J = f_J^2 - 1$ for the Jastrow correlation) and the BCS statistical correlations,

$$l_v(r) = \frac{\nu}{\rho_0} \int \frac{d^3 k}{(2\pi)^3} \exp(i\mathbf{k} \cdot \mathbf{r}) v^2(k), \quad (15)$$

$$l_u(r) = \frac{\nu}{\rho_0} \int \frac{d^3 k}{(2\pi)^3} \exp(i\mathbf{k} \cdot \mathbf{r}) u(k) v(k), \quad (16)$$

where ν is the spin–isospin degeneracy ($\nu = 2$ for PNM) and ρ_0 is the average density of the uncorrelated BCS model, given by

$$\rho_0 = \nu \int \frac{d^3k}{(2\pi)^3} v^2(k). \quad (17)$$

The FHNC equations, derived in I, sum at all orders the cluster diagrams contributing to $g(r_{12})$ and $n(r_{11'})$ in the Jastrow case. Here we are dealing with a spin–dependent correlation operator of the type \hat{F}_6 of Eq. (3), reduced to the PNM case.

In addition to the complexity introduced by the spin–dependence, the noncommutativity of $\hat{f}(ij)$ with $\hat{f}(ik)$ implies that any given cluster diagram generates as many clusters as the number of possible ordering of the operators presented in the diagram. This is a formidable task, which is not been yet solved. Reasonable approximations have been devised [19, 27] to sum up the leading cluster terms. Instead of following such schemes we calculate exactly the lowest order correlated cluster terms of $g(r_{12})$ and $n(r_{12} = 0)$. This is justified by the fact that we consider short–range correlations and a low density system. Moreover, we are mainly interested to derive the correlated BCS equations.

It is well known that normalization properties are better approximated by the successive terms of the power series expansion [28] namely the expansion in the number of correlation lines. The energy expectation value is instead better evaluated using the expansion in the number of particles, or, equivalently, in the density. Such inconsistency can be partially resolved by performing a full FHNC summation of both quantities in the case if the elementary diagrams give the negligible contributions. Here we will calculate $n(r_{12} = 0)$ up to the first order of PS expansion and $g(r_{12})$ at the two–body cluster level plus the vertex corrections, evaluated at the first order of the PS expansion, to be consistent with $n(r_{12} = 0)$.

A. One–body density and vertex corrections

For a BCS–type trial function the density is given by:

$$\rho = \frac{\langle \hat{N} \rangle}{\Omega} = \frac{\sum_m \langle a_m^\dagger a_m \rangle}{\Omega}. \quad (18)$$

Fluctuations with respect to this average vanish in the thermodynamic limit. We stress that the actual density, ρ , differs from ρ_0 because the correlation operator affects $\langle \hat{N} \rangle$ (see I). Therefore, ρ_0 has to be considered as a *variational* parameter, and ρ has to be computed self–consistently.

The calculation of ρ follows the FHNC scheme of I. We limit our attention to the FHNC diagrams with zero and one correlation lines, e.g. those belonging to the first order of the Power Series cluster expansion, Fig. (1) shows the first order diagrams.

The external point, denoted as 1, is represented by an open dot, whereas the internal points are given as black dots. The oriented lines represent exchange l_u or l_v functions, composed as in I, whereas the dashed ones are dynamical correlations $\hat{F}^2 - 1$. Diagram $D4$ has an overall $1/2$ symmetry factor, canceling the 2 factor coming from the two exchange loops with opposite orientations.

In the standard FHNC theory for the normal phase, diagrams $D1$ – $D4$ add up to give zero contribution: $D1$ is canceled by $D3$ and $D2$ by $D4$. We are left with the uncorrelated zeroth order diagrams, given rise to the Fermi gas momentum distribution, $n_k = \Theta(k_F - k)$, $k_F = (6\pi^2\rho/\nu)^{1/3}$ being the Fermi momentum. The total density correctly coincides, at any order of the power series, with that of the uncorrelated Fermi sea, $\rho = \rho_0$.

In correlated BCS theory this cancellation no longer holds, and corrections to the uncorrelated ρ_0 are found, namely $\rho \neq \rho_0$.

Following the notation of I, diagram $D1$ is the first order of the vertex correction of the U_d type, and the other three diagrams are included into the vertex correction of the U_e type. Keeping only the linear terms, the density ρ is given by

$$\rho \sim \rho_1 = c_d \rho_0, \quad (19)$$

where c_d is given, in terms of the cluster terms U_d and U_e , by the following equations:

$$\begin{aligned} c_e &= 1 + U_d, \\ c_d &= c_e + U_e = 1 + U_d + U_e. \end{aligned} \quad (20)$$

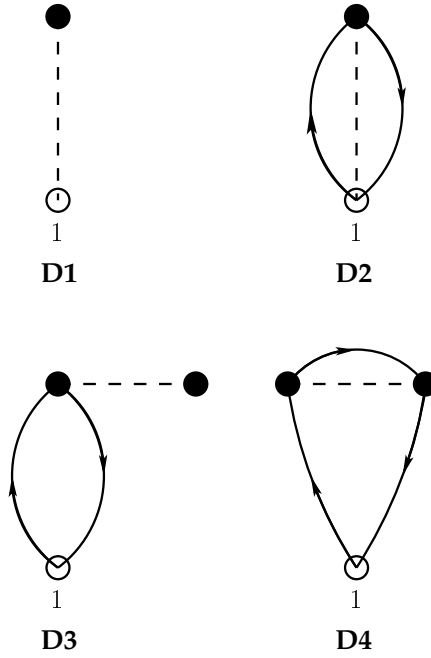


FIG. 1: The lowest order diagrams that contribute to the vertex corrections.

Accordingly, c_e is the correction to vertices which are arrival points of some exchange lines, whereas the complete c_d is the correction for vertices only connected to dynamical lines.

It is straightforward to extend the algebraic methods given in I to the case of the spin-dependent correlations.

We will now discuss the terms associated with the diagrammatic structures (D1–D4), contributing to U_d and U_e . For D1 we get:

$$D1 \rightarrow U_d = \rho_0 \int d^3 r \sum_{i,j} K^{ij1} \left(f^{(i)}(r) f^{(j)}(r) - \delta_{i1} \delta_{j1} \right). \quad (21)$$

The K^{ijk} matrix is given by

$$K^{ij1} = \begin{pmatrix} 1 & 0 & 0 \\ 0 & 3 & 0 \\ 0 & 0 & 6 \end{pmatrix}, \quad K^{ij2} = \begin{pmatrix} 0 & 1 & 0 \\ 1 & -2 & 0 \\ 0 & 0 & 2 \end{pmatrix}, \quad K^{ij3} = \begin{pmatrix} 0 & 0 & 1 \\ 0 & 0 & 1 \\ 1 & 1 & -2 \end{pmatrix}. \quad (22)$$

Two terms are associated to D3: the first term has both l_v -type exchange lines; in the second term one line is of the l_u -type. The total contribution is:

$$D3 \rightarrow U_{e3} = -U_d \frac{\nu}{\rho_0} \int \frac{d^3 k}{(2\pi)^3} (v^4(k) - u^2(k)v^2(k)). \quad (23)$$

In the normal phase, $u(k)v(k) = 0$ and $v^2(k) = \Theta(k_F - k)$, and $U_d + U_{e3} = 0$.

Similarly to D3, D2 has two analogous terms:

$$D2 \rightarrow U_{e2} = U_{e2}^v + U_{e2}^u, \quad (24)$$

where

$$U_{e2}^v = -\frac{\rho_0}{\nu} \int d^3 r l_v^2(r) \sum_{i,j,k} K^{ijk} A^k P_k \left(f^{(i)}(r) f^{(j)}(r) - \delta_{i1} \delta_{j1} \right), \quad (25)$$

$$U_{e2}^u = \frac{\rho_0}{\nu} \int d^3 r l_u^2(r) \sum_{i,j,k} K^{ijk} A^k B_k \left(f^{(i)}(r) f^{(j)}(r) - \delta_{i1} \delta_{j1} \right), \quad (26)$$

with $A^k = (1, 3, 6)$, $P_k = (1, 1, 0)$ and $B_k = (1, -1, 0)$ (note that the factor 1/2 of the spin-exchange operator is included in the factor in front of the integrals).

Diagram D4 has three different exchange patterns giving the contributions:

(i) U_{e4}^{vv} , having all l_v -type exchanges,

$$U_{e4}^{vv} = \frac{\rho_0}{\nu} \int d^3r l_v(r) l_{vv}(r) \sum_{i,j,k} K^{ijk} A^k P_k \left(f^{(i)}(r) f^{(j)}(r) - \delta_{i1} \delta_{j1} \right), \quad (27)$$

with,

$$l_{vv}(r) = \frac{\nu}{\rho_0} \int \frac{d^3k}{(2\pi)^3} \exp(i\mathbf{k} \cdot \mathbf{r}) v^4(k). \quad (28)$$

Again, if $v^2(k) = \theta(k_F - k)$, then $U_{e2}^v + U_{e4}^{vv} = 0$.

(ii) U_{e4}^{uu} , having two l_u exchanges joining at the external point 1, while the third exchange line is of the l_v -type,

$$U_{e4}^{uu} = -U_{e2}^v - U_{e4}^{vv} \quad (29)$$

(iii) U_{e4}^{uv} , having a l_u exchange joining with a l_v one at point 1, the third line being of the l_u -type,

$$U_{e4}^{uv} = \frac{\rho_0}{\nu} \int d^3r l_u(r) l_{uv}(r) \sum_{i,j,k} K^{ijk} A^k B_k \left(f^{(i)}(r) f^{(j)}(r) - \delta_{i1} \delta_{j1} \right), \quad (30)$$

with,

$$l_{uv}(r) = \frac{\nu}{\rho_0} \int \frac{d^3k}{(2\pi)^3} \exp(i\mathbf{k} \cdot \mathbf{r}) u(k) v^3(k). \quad (31)$$

The total U_{e4} term is the sum

$$U_{e4} = U_{e4}^{vv} + U_{e4}^{uu} + 2U_{e4}^{uv}. \quad (32)$$

In conclusion, U_e is given by:

$$U_e = U_{e2} + U_{e3} + U_{e4} = U_{e2}^u + U_{e3} + 2U_{e4}^{uv}. \quad (33)$$

B. Potential energy

We perform the calculation of the expectation value of a v_6 potential at the two-body order for the cluster expansion, but including also the vertex corrections at the interaction points, 1 and 2. The reason for going beyond the simple two-body approximation in the superfluid phase lies in the correlation driven modification of the expectation value of the number operator with respect to BCS, as discussed in the previous subsection.

The vertex corrections lead to a fully factorized term, similar to that in the Jastrow correlated BCS case of I, plus commutator correction terms,

$$\begin{aligned} \frac{\langle \hat{V} \rangle_2}{\langle \hat{N} \rangle_1} &= V_2 = \frac{\rho}{2} \int d^3r_{12} \left[V_d(r_{12}) - \frac{1}{\nu} \left(\frac{c_e}{c_d} \right)^2 [V_{ev}(r_{12}) l_v^2(r_{12}) - V_{eu}(r_{12}) l_u^2(r_{12})] \right] \\ &+ \Delta C_d + \Delta C_{ev} + \Delta C_{eu}, \end{aligned} \quad (34)$$

where the ΔC terms are the commutator corrections.

The V_d and V_{ev} functions coincide with the direct and exchange terms of the normal phase of PW,

$$\begin{aligned} V_d(r) &= \sum_{i,j,k} f^{(i)}(r) v^{(j)}(r) f^{(k)}(r) K^{ijk} A^k, \\ V_{ev}(r) &= \sum_{i,j,j',k,l} f^{(i)}(r) v^{(j)}(r) f^{(k)}(r) K^{ijj'} K^{j'kl} A^l P_l. \end{aligned} \quad (35)$$

After performing the spin algebra corresponding to the last term of the first line of (34), we obtain

$$V_{eu}(r) = \sum_{i,j,j',k,l} f^{(i)}(r)v^{(j)}(r)f^{(k)}(r)K^{ijj'}K^{j'kl}A^lB_l. \quad (36)$$

All the vertex structures $D1$ – $D4$ contribute to c_d , as discussed in the previous subsection. However, only $D1$ and $D2$ originate commutator contributions.

The commutator terms ΔC are calculated following the algebraic methods of ref. [19]. After some lengthy calculations we obtain:

$$\begin{aligned} \Delta C_d &= -(\bar{U}_d - \bar{U}_{e2}^v + \bar{U}_{e2}^u)\rho_0 \int d^3r_{12} \\ &\quad \times \sum_{i,j,k} K^{ijk}A^k(3 - \delta_{i1} - \delta_{j1} - \delta_{k1})f^{(i)}(r_{12})v^{(j)}(r_{12})f^{(k)}(r_{12}), \end{aligned} \quad (37)$$

$$\begin{aligned} \Delta C_{ev} &= \bar{U}_d \frac{\rho_0}{\nu} \int d^3r_{12} l_v^2(r_{12}) \\ &\quad \times \sum_{i,j,j',k,l} K^{ijj'}K^{j'kl}A^lP_l(4 - 2\delta_{j'1} - \delta_{j1} - \delta_{l1})f^{(i)}(r_{12})v^{(j)}(r_{12})f^{(k)}(r_{12}), \end{aligned} \quad (38)$$

$$\begin{aligned} \Delta C_{eu} &= -\bar{U}_d \frac{\rho_0}{\nu} \int d^3r_{12} l_u^2(r_{12}) \\ &\quad \times \sum_{i,j,j',k,l} K^{ijj'}K^{j'kl}A^lB_l(4 - 2\delta_{j'1} - \delta_{j1} - \delta_{l1})f^{(i)}(r_{12})v^{(j)}(r_{12})f^{(k)}(r_{12}). \end{aligned} \quad (39)$$

where

$$\bar{U}_d = \frac{\rho_0}{3} \int d^3r_{13} \sum_{i=2,3} A^i f^{(i)}(r_{13}) f^{(i)}(r_{13}), \quad (40)$$

$$\bar{U}_{e2}^v = -\frac{\rho_0}{\nu} \int d^3r_{13} l_v^2(r_{13}) \left(f^{(1)}(r_{13})f^{(2)}(r_{13}) - f^{(1)}(r_{13})f^{(1)}(r_{13}) + 4f^{(3)}(r_{13})f^{(3)}(r_{13}) \right), \quad (41)$$

$$\bar{U}_{e2}^u = -\frac{3\rho_0}{\nu} \int d^3r_{13} l_u^2(r_{13}) f^{(2)}(r_{13}) f^{(2)}(r_{13}). \quad (42)$$

These expressions sum the commutator corrections which are linear in the vertex corrections $D1$ and $D2$. The much smaller higher order terms have been disregarded.

C. Kinetic energy

We will adopt the Jackson–Feenberg (JF) identity to evaluate the kinetic energy [14]. The advantage of using this form lies in the fact that the JF kinetic energy operator is mainly constructed by the sum of one– and two–body operators, the three–body operators being almost negligible. Other forms, like the Pandharipande–Bethe or the Clark–Westhaus ones, have large three–body pieces, and need to go beyond our two–body plus vertex corrections approximation.

The kinetic energy expectation value per particle is given by the sum of a one– and a two–body term:

$$\frac{\langle \hat{T} \rangle_2}{\langle \hat{N} \rangle_1} = T_1 + T_2, \quad (43)$$

where T_1 gives the *uncorrelated* BCS kinetic energy per particle,

$$T_1 = \frac{\hbar^2}{2m} \frac{\nu}{\rho} \int \frac{d^3k}{(2\pi)^3} k^2 v^2(k). \quad (44)$$

The JF T_2 energy is given by:

$$\begin{aligned} T_2 &= -\frac{\hbar^2}{4m} \rho \int d^3r_{12} \left[T_d^{JF}(r_{12}) - \frac{1}{\nu} \left(\frac{c_e}{c_d} \right)^2 [T_{ev}^{JF}(r_{12})l_v^2(r_{12}) - T_{eu}^{JF}(r_{12})l_u^2(r_{12})] \right. \\ &\quad \left. - \frac{1}{2} (T_{2v}^{JF}(r_{12})\nabla^2 l_v^2(r_{12}) - T_{2u}^{JF}(r_{12})\nabla^2 l_u^2(r_{12})) \right] + \Delta T_d + \Delta T_{ev} + \Delta T_{eu}. \end{aligned} \quad (45)$$

T_d and T_{ev} , corresponding to the direct and exchange terms of the normal case, are:

$$\begin{aligned} T_d^{JF}(r_{12}) &= \sum_i A^i \left(f^{(i)}(r_{12}) \nabla^2 f^{(i)}(r_{12}) - (\vec{\nabla} f^{(i)}(r_{12}))^2 \right), \\ T_{ev}^{JF}(r_{12}) &= \sum_{i,k,l} K^{ikl} A^l P_l \left(f^{(i)}(r_{12}) \nabla^2 f^{(k)}(r_{12}) - \vec{\nabla} f^{(i)}(r_{12}) \cdot \vec{\nabla} f^{(k)}(r_{12}) \right), \\ T_{2v}^{JF}(r_{12}) &= \sum_{i,k,l} K^{ikl} A^l P_l \left(f^{(i)}(r_{12}) f^{(k)}(r_{12}) - \delta_{i1} \delta_{k1} \right). \end{aligned} \quad (46)$$

Similarly, the u -terms are:

$$\begin{aligned} T_{eu}^{JF}(r_{12}) &= \sum_{i,k,l} K^{ikl} A^l B_l \left(f^{(i)}(r_{12}) \nabla^2 f^{(k)}(r_{12}) - \vec{\nabla} f^{(i)}(r_{12}) \cdot \vec{\nabla} f^{(k)}(r_{12}) \right), \\ T_{2u}^{JF}(r_{12}) &= \sum_{i,k,l} K^{ikl} A^l B_l \left(f^{(i)}(r_{12}) f^{(k)}(r_{12}) - \delta_{i1} \delta_{k1} \right). \end{aligned} \quad (47)$$

The commutators terms are calculated as for the potential:

$$\Delta T_d = \frac{\hbar^2}{2m} (\bar{U}_d - \bar{U}_{e2}^v + \bar{U}_{e2}^u) \rho_0 \int d^3 r_{12} \sum_{i=2,3} A^i \left(f^{(i)}(r_{12}) \nabla^2 f^{(i)}(r_{12}) - (\vec{\nabla} f^{(i)}(r_{12}))^2 \right), \quad (48)$$

$$\begin{aligned} \Delta T_{ev} &= -\frac{\hbar^2}{2m} \bar{U}_d \frac{\rho_0}{\nu} \int d^3 r_{12} \sum_{i,k,l} K^{ikl} A^l P_l (3 - \delta_{i1} - \delta_{k1} - \delta_{l1}) \\ &\times \left(\left(f^{(i)}(r_{12}) \nabla^2 f^{(k)}(r_{12}) - \vec{\nabla} f^{(i)}(r_{12}) \cdot \vec{\nabla} f^{(k)}(r_{12}) \right) l_v^2(r_{12}) - \frac{1}{2} f^{(i)}(r_{12}) f^{(k)}(r_{12}) \nabla^2 l_v^2(r_{12}) \right), \end{aligned} \quad (49)$$

$$\begin{aligned} \Delta T_{eu} &= \frac{\hbar^2}{2m} \bar{U}_d \frac{\rho_0}{\nu} \int d^3 r_{12} \sum_{i,k,l} K^{ikl} A^l B_l (3 - \delta_{i1} - \delta_{k1} - \delta_{l1}) \\ &\times \left(\left(f^{(i)}(r_{12}) \nabla^2 f^{(k)}(r_{12}) - \vec{\nabla} f^{(i)}(r_{12}) \cdot \vec{\nabla} f^{(k)}(r_{12}) \right) l_u^2(r_{12}) - \frac{1}{2} f_i^{(i)}(r_{12}) f_k^{(k)}(r_{12}) \nabla^2 l_u^2(r_{12}) \right). \end{aligned} \quad (50)$$

We disregard the small three-body contributions to the JF kinetic energy. As for the potential energy, the commutator terms include only cluster diagrams which are linear in the vertex corrections.

The energy expectation value, at the two-body order of the cluster expansion, is:

$$E_2 = \frac{\langle \hat{H} \rangle_2}{\langle \hat{N} \rangle_1} = T_1 + T_2 + V_2. \quad (51)$$

III. EULER AND CORRELATED GAP EQUATIONS

The Euler and the correlated gap equations form a set of coupled equations, whose solution determines the correlation functions and the correlated BCS amplitudes. They result from the variational requirement:

$$\delta_{v,f^{(i)}} \langle \hat{H} - \lambda \hat{N} \rangle = 0. \quad (52)$$

In deriving the equations we will use the two-body approximation previously discussed,

$$\begin{aligned} \langle \hat{H} \rangle &\sim \langle \hat{H} \rangle_2, \\ \langle \hat{N} \rangle &\sim \langle \hat{N} \rangle_1 = \Omega \rho, \end{aligned} \quad (53)$$

where E_2 and ρ_1 are given in Eqs. (51) and (19), respectively.

We will make further approximations, which we believe are accurate enough, but that can be eventually released. They consist of:

- (i) neglecting the commutator terms in the derivation of the Euler equation, while keeping them in the calculation of E_2 and ρ_1 ;

- (ii) decoupling the BCS amplitude, $v(q)$, from the correlation functions, $f^{(i)}(r)$. As a consequence, we neglect the implicit dependence on $f^{(i)}(r)$ in the functional variation with respect to $v(q)$, and viceversa in the derivation of the Euler equations for $f^{(i)}(r)$.

In this way we arrive at an Euler equation of *precisely* the same algebraic structure as that of the bare BCS scheme, with the Hamiltonian containing paired terms only [29]. However, with respect to the ordinary BCS treatment, there is the crucial distinction that the pairing force and the single-particle energies are now *renormalized* by the dynamical correlations. Correlations also affect the mean density through the vertex corrections of the BCS/FHNC theory. The explicit formulae are given below.

A. Euler equations for the correlation functions

Following the PW notation for standard nuclear matter, where the Schrödinger-like equations are written in the T, S channels (here we consider the isospin $T = 1$ channel only), the following changes are made with respect to the normal phase equations:

($S = 0$): in the singlet channel, eq. (3.12) of PW,

$$\Phi_{S=0,T=1} \rightarrow \sqrt{1 + \left(\frac{c_e}{c_d}\right)^2 (l_v^2(r) + 2l_u^2(r))}. \quad (54)$$

($S = 1$): in the triplet channel, eq. (3.14) of PW,

$$\Phi_{S=1,T=1} \rightarrow \sqrt{1 - \left(\frac{c_e}{c_d}\right)^2 l_v^2(r)}. \quad (55)$$

The modifications to the spin-orbit equations are not included since we are dealing with a v_6 model.

B. Correlated gap equation

The correlated gap equations is derived from:

$$\delta_{v(k)}(\rho E_2 - \rho\lambda) = 0. \quad (56)$$

The functional variation of the density is given by:

$$\delta_{v(k)}\rho = (1 + U_d + U_e)\delta_{v(k)}\rho_0 + \rho_0\delta_{v(k)}(U_d + U_e), \quad (57)$$

where

$$\delta_{v(k)}\rho_0 = \rho_0 \frac{\nu k^2}{2\pi^2 \rho_0} (2v(k)\delta v_k). \quad (58)$$

After performing the tedious variations of the vertex terms, U_d and U_e , we arrive at the expression:

$$\delta_{v(k)}\rho = \tilde{E}_0(k) (\delta_{v(k)}\rho_0), \quad (59)$$

where

$$\begin{aligned} \tilde{E}_0(k) &= \frac{\delta_{v(k)}\rho}{\delta_{v(k)}\rho_0} = 1 + U_d(3 - 4v^2(k)) + U_e 3 \\ &+ \frac{2 - v^2(k) - 4v^4(k)}{2u(k)v(k)} \int \frac{d^3q}{(2\pi)^3} F_u(q)u(|\mathbf{k} - \mathbf{q}|)v(|\mathbf{k} - \mathbf{q}|) \\ &+ \frac{1 - 2v^2(k)}{2u(k)v(k)} \int \frac{d^3q}{(2\pi)^3} F_u(q)u(|\mathbf{k} - \mathbf{q}|)v^3(|\mathbf{k} - \mathbf{q}|), \end{aligned} \quad (60)$$

and $F_u(q)$ is

$$F_u(q) = \int d^3r \exp(i\mathbf{q} \cdot \mathbf{r}) \sum_{i,k,l} K^{ikl} A^l B_l (f_i(r) f_k(r) - \delta_{i1} \delta_{k1}) . \quad (61)$$

The variation of ρ plays a role in:

- (i) the term $\rho\lambda$ of Eq. (57), giving rise to $\lambda\tilde{E}_0(q)$ ($\delta_{v(k)}\rho_0$);
- (ii) the direct term of $\rho E_2 \rightarrow \rho E_d$, where

$$\rho E_d = \frac{\rho^2}{2} \int d^3r_{12} \left(V_d(r_{12}) - \frac{\hbar^2}{2m} T_d(r_{12}) \right) . \quad (62)$$

In this case we get: $2E_d\tilde{E}_0$ ($\delta_{v(k)}\rho_0$);

- (iii) the exchange term of $\rho E_2 \rightarrow \rho E_e$, where

$$\begin{aligned} \rho E_e = & -\frac{1}{2\nu} (c_e \rho_0)^2 \int d^3r_{12} \left\{ (V_{ev}(r_{12}) l_v^2(r_{12}) - V_{eu}(r_{12}) l_u^2(r_{12})) \right. \\ & - \frac{\hbar^2}{2m} [T_{ev}(r_{12}) l_v^2(r_{12}) - T_{eu}(r_{12}) l_u^2(r_{12}) \\ & \left. - \frac{1}{2} (T_{2v}(r_{12}) \nabla^2 l_v^2(r_{12}) - T_{2u}(r_{12}) \nabla^2 l_u^2(r_{12}))] \right\} . \end{aligned} \quad (63)$$

This variation applies to the $l_v(r)$ and $l_u(r)$ functions appearing in E_e , with the result

$$\delta_{v(k)}(\rho E_e) = \left\{ \Sigma(k) - \Delta(k) \frac{1 - 2v^2(k)}{2u(k)v(k)} \right\} (\delta_{v(k)}\rho_0) , \quad (64)$$

where

$$\begin{aligned} \Sigma(k) = & -c_e^2 \int \frac{d^3q}{(2\pi)^3} v^2(|\mathbf{k} - \mathbf{q}|) \left(V_{ev}^T(q) - \frac{\hbar^2}{2m} \left(T_{ev}^T(q) + \frac{q^2}{2} T_{2v}^T(q) \right) \right) \\ & + 2 \frac{c_e - 1}{c_e} (c_d E_e) , \end{aligned} \quad (65)$$

$$\Delta(k) = -c_e^2 \int \frac{d^3q}{(2\pi)^3} u(|\mathbf{k} - \mathbf{q}|) v(|\mathbf{k} - \mathbf{q}|) \left(V_{eu}^T(q) - \frac{\hbar^2}{2m} \left(T_{eu}^T(q) + \frac{q^2}{2} T_{2u}^T(q) \right) \right) , \quad (66)$$

where $V_{ev}^T(q)$ and $V_{eu}^T(q)$ are the Fourier transforms of $V_{ev}(r)$ and $V_{eu}(r)$ of Eqs. (35) and (36), respectively. Similarly, $T_{ev}^T(q)$ and $T_{2v}^T(q)$ are the Fourier transforms of $T_{ev}^{JF}(r)$ and $T_{2v}^{JF}(r)$ of Eq. (46); $T_{eu}^T(q)$ and $T_{2u}^T(q)$ are the Fourier transforms of $T_{eu}^{JF}(r)$ and $T_{2u}^{JF}(r)$ of Eq. (47).

Notice that $\Sigma(k)$, of Eq. (65), includes the constant term provided by the functional variation of the vertex correction.

After collecting all the terms, we may write a correlated gap equation, or Euler equation for the correlated BCS amplitudes, in the form:

$$\left(\frac{\hbar^2 k^2}{2m} - \bar{\lambda} \tilde{E}_0(k) \right) v(k) + \Sigma(k) v(k) - \Delta(k) \frac{1 - 2v^2(k)}{2\sqrt{1 - v^2(k)}} = 0 , \quad (67)$$

which resembles that obtained in standard BCS theory [29]. The solution for $v^2(k)$ of the correlated gap equation can be written as:

$$v^2(k) = \frac{1}{2} \left(1 - \frac{\epsilon(k)}{E(k)} \right) , \quad (68)$$

with

$$\epsilon(k) = \frac{\hbar^2 k^2}{2m} + \Sigma(k) - \bar{\lambda} \tilde{E}_0(k) , \quad (69)$$

$$E(k) = \sqrt{\Delta^2(k) + \epsilon^2(k)} , \quad (70)$$

$$\bar{\lambda} = \lambda - 2E_d , \quad (71)$$

where $\Delta(k)$ has to be interpreted as the *correlated* gap function. Its value at $k = k_F$, Δ_F , is the energy gap, namely the energy required to break a pair at the Fermi surface. In the present case, the functions $\tilde{E}_0(k)$, $\Sigma(k)$ and $\Delta(k)$ all depend upon $v^2(k)$, making the correlated gap equation (68) highly non linear.

C. Correlated versus standard BCS equation

The correlated BCS equation (68) has the same algebraic structure as the uncorrelated one (see ref. [29], Eqs. (5.29) and (5.30)). However, the standard BCS equations do not contain the $\Sigma(k)$ term, whereas in our approach $\Sigma(k) \neq 0$, even if the correlation operator is set equal to 1. In fact, in this case the quantities $\tilde{E}_0(k)$, $\Sigma(k)$ and $\Delta(k)$ become:

$$\begin{aligned}\tilde{E}_0(k) &\rightarrow 1, \\ \Sigma(k) &\rightarrow - \int \frac{d^3q}{(2\pi)^3} v^2(|\mathbf{k} - \mathbf{q}|) [v_c(q) + 3v_\sigma(q)], \\ \Delta(k) &\rightarrow - \int \frac{d^3q}{(2\pi)^3} u(|\mathbf{k} - \mathbf{q}|) v(|\mathbf{k} - \mathbf{q}|) [v_c(q) - 3v_\sigma(q)].\end{aligned}\quad (72)$$

In correlated BCS, $\Sigma(k)$ dresses the single particle energies $\hbar^2 k^2 / 2m$, and $\tilde{E}_0(k)$ renormalizes the mass. Similarly, $\Delta(k)$ assumes the role of the gap function. From Eq. (5.32) of ref. [29]

$$\Delta(k) = - \sum V_{\mathbf{k}\mathbf{q}} \frac{\Delta(q)}{2E(q)}, \quad (73)$$

where

$$V_{\mathbf{k}\mathbf{q}} = \int d^3r \exp(i(\mathbf{k} - \mathbf{q}) \cdot \mathbf{r}) V(r). \quad (74)$$

From Eq. (68) and the normalization relation, $u^2(k) + v^2(k) = 1$, it follows that

$$u(k)v(k) = \frac{1}{2} \sqrt{1 - \frac{\epsilon^2(k)}{E^2(k)}} = \frac{\Delta(k)}{2E(k)}. \quad (75)$$

Therefore

$$\Delta(k) = - \sum V_{\mathbf{k}\mathbf{q}} u(q)v(q), \quad (76)$$

coincides with Eq. (66).

The comparison with the uncorrelated BCS theory allows identifying $E(k)$ with the excitation energy of the broken pair (BP) with respect to the ground-state, as defined in Ref. [29],

$$E_{BP} - E_{GS} \equiv E(k). \quad (77)$$

IV. RESULTS

We have solved the BCS and correlated BCS equations for neutron matter with a variety of potentials, namely the Reid (R), Argonne v_{14} (A14) and Argonne $v_{s'}$ (A8') ones. In solving the gap equations we have generalized the method described by Khodel et al. in Ref. [30]. According to this method the original gap equation is identically replaced by a set of coupled equations: a non-singular quasilinear integral equation for the dimensionless profile function, $\chi(k)$, defined by $\Delta(k) = \chi(k) \Delta_F$ and a non-linear algebraic one for the gap, $\Delta_F = \Delta(k_F)$, at the Fermi surface. After integrating Eq. (66) over the angle, we obtain

$$\Delta(k) = -c_e^2 \int_0^\infty \frac{q^2 dq}{2\pi^2} \frac{V(k, q) \Delta(q)}{2\sqrt{\Delta^2(q) + \epsilon^2(q)}}, \quad (78)$$

with,

$$V(k, q) = 4\pi \int_0^\infty r^2 dr j_0(kr) \left\{ V_{eu}(r) - \frac{\hbar^2}{2m} \left[T_{eu}(r) + \frac{k^2 + q^2}{2} T_{2u}(r) \right] \right\} j_0(qr) + \frac{\hbar^2 kq}{2m} 4\pi \int_0^\infty r^2 dr j_1(kr) T_{2u}(r) j_1(qr). \quad (79)$$

It is assumed that the interaction $V(k, q)$ is different from zero at the Fermi surface, $V(k_F, k_F) \neq 0$. To solve the gap equation we decompose the potential, $V(k, q)$, into a separable part and a remainder, $W(k, q)$, that vanishes when either argument is at the Fermi surface:

$$V(k, q) = V_F \phi(k) \phi(q) + W(k, q), \quad (80)$$

where $W(k_F, k) = W(k, k_F) \equiv 0$ and $\phi(k) = V(k, k_F)/V_F$. Then, the gap equation (78) is readily seen to be equivalent to an integral equation for the shape function, $\chi(k)$,

$$\chi(k) + c_e^2 \int_0^\infty \frac{q^2 dq}{2\pi^2} \frac{W(k, q) \chi(q)}{2\sqrt{\Delta_F^2 \chi^2(q) + \epsilon^2(q)}} = \phi(k), \quad (81)$$

together with the *algebraic* equation,

$$1 + c_e^2 V_F \int_0^\infty \frac{q^2 dq}{2\pi^2} \frac{\chi(q) \phi(q)}{2\sqrt{\Delta_F^2 \chi^2(q) + \epsilon^2(q)}} = 0, \quad (82)$$

for the gap amplitude Δ_F (assumed nonzero). Since $W(k, k_F)$ is zero by construction, the integral equation (81) has a nonsingular kernel, the log-singularity of the BCS equation having been isolated in the amplitude equation (82). An iterative solution of this set of equations converges very rapidly.

The correlated gap equations are solved using the BCS solution at a given k_F as an input. We find that the final density, ρ , is always very close to the initial one, ρ_0 . The maximum difference between k_F^{input} and k_F^{final} is well below one percent. In Table (I) we show the input and output values of k_F , of the density, ρ , of the chemical potentials, λ_F , of the effective mass, m^*/m , defined by the relation:

$$\left(\frac{m^*}{m} \right)^{-1} = \frac{m}{\hbar^2} \left(\frac{1}{k} \frac{de(k)}{dk} \right)_{k=k_F}, \quad e(k) = \frac{\hbar^2 k^2}{2m} + \Sigma(k), \quad (83)$$

and of the gap Δ_F obtained with the A8' model for the uncorrelated BCS, and for the Jastrow (J) and f_6 correlated (CO) cases.

It is evident that the introduction of the correlations very slightly affects the total density. On the contrary the chemical potential is reduced by the Jastrow correlations by ~ 20 to $\sim 30\%$. Spin dependent correlations provide a further, even if small, decrease of $\lambda_F = \hbar^2 k_F^2 / 2m$. The effective mass, computed via the self-energy $\Sigma(k)$, considerably decreases after the introduction of the correlations. The normal phase effective mass, computed microscopically in CBF, at $k_F = 0.8 \text{ fm}^{-1}$ is ~ 0.8 .

In Figure (2) we show the Jastrow, spin and tensor correlations at $k_F = 0.6 \text{ fm}^{-1}$ for the A8' potential. The dash-dotted lines are the normal phase correlations, whereas the solid lines give the correlations after solving the correlated gap equations. For the S -pairing case Jastrow and tensor correlations do not change from the normal to the BCS phases. Instead, the spin correlation shows some sensitivity to the environmental phase. It is reasonable to expect that for the 3P_2 - 3F_2 pairing the tensor correlation also will depend on the phase.

The u^2 , $2uv$ and v^2 amplitudes, both for the pure and correlated BCS cases, are shown in Figure (3) at three Fermi momenta. At the lowest value, $k_F = 0.1 \text{ fm}^{-1}$, the uncorrelated and correlated amplitudes substantially differ among each other, the correlated ones showing a larger deviation from the step function, consistent with the larger gap value ($\Delta_F^0 = 0.07 \text{ MeV}$ and $\Delta_F^{CO} = 0.14 \text{ MeV}$). At $k_F = 0.6 \text{ fm}^{-1}$ the amplitudes are very close in both approaches, yielding similar gaps ($\Delta_F^0 = 2.27 \text{ MeV}$ and $\Delta_F^{CO} = 2.25 \text{ MeV}$). At the largest value, $k_F = 0.8 \text{ fm}^{-1}$, the correlated amplitudes are practically step functions. In fact this is almost the highest density for which we find solution to the correlated BCS equations.

The gap function, $\Delta(k)$, at $k_F = 0.6 \text{ fm}^{-1}$ is given in Figure (4). In addition to the pure and correlated BCS functions, we show the one obtained by a simple Jastrow-correlated wave-function. At low k -values, $k/k_F < 2.5$, the effects of the Jastrow and spin-dependent correlations compensate, providing a gap function close to the BCS result.

At larger momenta they add and the correlated gap function departs from the uncorrelated one, up to $k/k_F \sim 15$, where all functions have essentially vanished.

The self-energy, $\Sigma(k)$, is depicted in Figure (5) at $k_F = 0.6 \text{ fm}^{-1}$. The main difference between the BCS and correlated BCS cases lies in the sharp rising of the correlated $\Sigma(k)$ at $k \sim k_F$, which produces the much lower effective mass given in Table (I), $(m^*/m)^0 = 0.96$ and $(m^*/m)^{\text{CO}} = 0.62$. The mass renormalization, caused by short-range correlations, enhanced the dispersive effect of the mean field, which leads to quenching of the energy gap, which is enhanced by the screening effect of the neutron pairing potential.

Figure (6) displays the energy gap at the Fermi surface, $\Delta_F^{(0)}$, as a function of the Fermi momentum for the A8' potential in the uncorrelated BCS case. The curves correspond to the full and to the decoupling approximation solutions of Ref. [16, 31], with and without the self-energy insertions of eq. (72). The two gaps are very close for $\Sigma(k) = 0$, whereas, after the introduction of the self-energy, the decoupling approximation appears to slightly overestimate the full solution.

Figure (7) gives the gaps for different types of correlations (Jastrow and f_6) and at various levels of the cluster expansion for the same potential. The Δ^0 gaps are the standard BCS results, those with the superscript 'J' are obtained within the Jastrow correlated theory and the 'CO' superscript denotes the corresponding correlations. The 2b and 3b subscripts in the correlated gaps refer to the pure two-body cluster case and to the one in which the density and the vertex corrections are computed at the first order of the power series expansion of Fig. (1). The inclusion of the Jastrow and f_6 correlations in the 2b case enhance the gap, because the short-range repulsion of the potential is renormalized by the short-range correlations. The 3b cases include medium modification effects via higher order cluster terms. Their effect is quite sizeable and reverse the behavior, both reducing the density region where we find a BCS solution and decreasing the maximum gap with respect to the standard case for the spin-dependent correlations. In fact, $\Delta^0(\text{max}) \sim 2.6 \text{ MeV}$ at $k_F \sim 0.9 \text{ fm}^{-1}$, while $\Delta_{f_6}^{3b}(\text{max}) \sim 2.2 \text{ MeV}$ at $k_F \sim 0.6 \text{ fm}^{-1}$. These results indicate that higher order many-body cluster terms may be relevant to estimate the gap.

Finally, in Figure (8) we show the gaps for different potentials in the BCS and f_6 -correlated theories. We have used, besides the Argonne $v_{8'}$ model, also the Reid and Argonne v_{14} (A14) potentials. These potentials differ mostly for the strength of the one-pion exchange induced components. In fact, A14 has much stronger spin and tensor potentials than Reid and A8'. This difference shows up in the gaps, in both approaches. The BCS gap is larger in A14 than for the other potentials, and more drastically reduced in the correlated case, where $\Delta_{\text{A14}}(\text{max}) \sim 1.7 \text{ MeV}$ at $k_F \sim 0.5 \text{ fm}^{-1}$.

Our results for the A14 potential are qualitatively similar to those of Ref. [32] (see also Ref. [33], where the more recent calculations was done), where the medium polarization was included via Landau theory. The authors found an analogous decrease of the BCS gap, with $\Delta_{\text{A14}}^{\text{Landau}}(\text{max}) \sim 1.5 - 2 \text{ MeV}$ at $k_F \sim 0.8 \text{ fm}^{-1}$, but with a wider density region allowing for a superfluid solution.

V. CONCLUSIONS AND PERSPECTIVES

The problem of an accurate determination of the BCS gap in a strongly interacting matter of nucleons is a long-standing one. Medium modification effects are expected to be important, but of difficult quantitative evaluation. We have used FHNC/BCS theory to take care of the short range correlations induced by the interaction in neutron matter at zero temperature. We have adopted the realistic Argonne $v_{8'}$ two-nucleon potential and a correlation factor having central, spin and tensor dependent components. The density has been computed at the first order of the power series expansion, since this expansion provides at each order the correct density normalization in the normal phase. Consistently, the matrix elements of the hamiltonian in the correlated BCS state are evaluated at the two-body cluster level plus vertex corrections at the interacting pair. This treatment, in conjunction with the use of spin and tensor correlations lowers the maximum gap at k_F by $\sim 20\%$ with respect to the uncorrelated BCS case. Moreover, Δ_F is shifted to a lower density. It is clear from our results the relevance of state dependent correlations for a reliable estimate of Δ_F in neutron matter, as well as the need for inserting medium modifications via higher order terms of the cluster expansion. Simple Jastrow, spin independent correlations always enhance Δ_F , even if massive summations of cluster diagrams are performed. This effect is due to the screening of the short-range repulsive interaction provided by the Jastrow correlations. Similar conclusions are drawn when the short-range correlations are introduced by medium effects within the Brueckner G-matrix theory. State dependent correlations reverse this scenario and, after the inclusion of the vertex corrections, reduce Δ_F . A qualitatively analogous result is found when state dependence is introduced by a CBF based perturbative expansion theory on top of Jastrow correlated states, but with spin dependent interactions.

In conclusion, we have stressed in this paper the importance of state dependent correlations and medium effects in superfluid neutron matter. Both of these tend to reduce the 1S_0 pairing gap, confirming previous studies.

k_F^0	[fm ⁻¹]	0.1	0.2	0.3	0.4	0.5	0.6	0.7	0.8	0.9	1.0	1.1	1.2	1.3
ρ_0	[fm ⁻³]	.000034	.00027	.00091	.00216	.00422	.00730	.01158	.01729	.02462	.03377	.04495	.05836	.07420
λ_F^0	[MeV]	.1780	.6615	1.4771	2.6628	4.2509	6.2696	8.7478	11.721	15.239	19.379	24.254	30.030	36.907
$(m^*/m)^0$.9994	.9960	.9897	.9811	.9708	.9589	.9452	.9296	.9120	.8926	.8716	.8496	.8270
Δ_F^0	[MeV]	.0719	.3568	.7986	1.3188	1.8359	2.2719	2.5576	2.6391	2.4850	2.0963	1.5209	.8713	.3247
k_F^J	[fm ⁻¹]	.1001	.2002	.3006	.4011	.5020	.6030	.7041	.8049	.9048	1.0032			
ρ_J	[fm ⁻³]	.000034	.00027	.00092	.00218	.00427	.00741	.01179	.01761	.02502	.03410			
λ_F^J	[MeV]	.1289	.5100	1.1721	2.0775	3.2336	4.6656	6.3312	8.2222	10.3590	12.737			
$(m^*/m)^J$.9774	.9480	.9072	.8609	.8065	.7370	.6516	.5426	.4035	.2591			
Δ_F^J	[MeV]	.1319	.5067	1.0236	1.6511	2.2785	2.7398	2.9884	2.9373	2.5069	1.6666			
k_F^{CO}	[fm ⁻¹]	.1001	.2002	.3006	.4011	.5017	.6022	.7020	.8004					
ρ_{CO}	[fm ⁻³]	.000034	.00027	.00092	.00218	.00427	.00738	.01168	.01732					
λ_F^{CO}	[MeV]	.1204	.4808	1.0709	1.8602	2.8082	3.8527	4.9220	5.9532					
$(m^*/m)^{CO}$.9787	.9470	.9023	.8409	.7533	.6146	.3997	.2476					
Δ_F^{CO}	[MeV]	.1379	.5104	1.0291	1.5861	2.0471	2.2487	1.9257	0.7098					

TABLE I: Fermi momentum, k_F , density, ρ , chemical potential, λ_F , effective mass, m^*/m , and gap value, Δ_F , in different approximations (see text).

The large effects found either by extending the study to the full FHNC/SOC calculations or after the introduction of the vertex corrections, strongly point to the need of a realistic estimate of many body effects. This can be done by using the calculated correlated BCS amplitudes as the guiding function of an AFDMC calculation. In the latter approach it is crucial to have a realistic guiding function in the path constraint. An extension of AFDMC to deal with the superfluid phases of neutron matter has been recently made and preliminary results, obtained for 14 neutrons, are given in Ref. [25]. A full description of both the AFDMC/BCS method and the corresponding results obtained for large systems will be given in a forthcoming paper [34]. An important issue is the role of the long range correlations. This can be most easily done in a Jastrow correlated BCS case. Work in this direction is in progress.

Acknowledgments

This work has been partially supported by the Italian MIUR through the PRIN: *Fisica Teorica del Nucleo Atomico e dei Sistemi a Molti Corpi*. K.E.S. acknowledges partial support by the US National Science Foundation via grant PHY-0456609. A.Yu.I. is grateful to INFN and to the Dipartimento di Fisica "E.Fermi" of the University of Pisa and acknowledges partial support from the PRIN 2006 *Quantum noise in mesoscopic systems*.

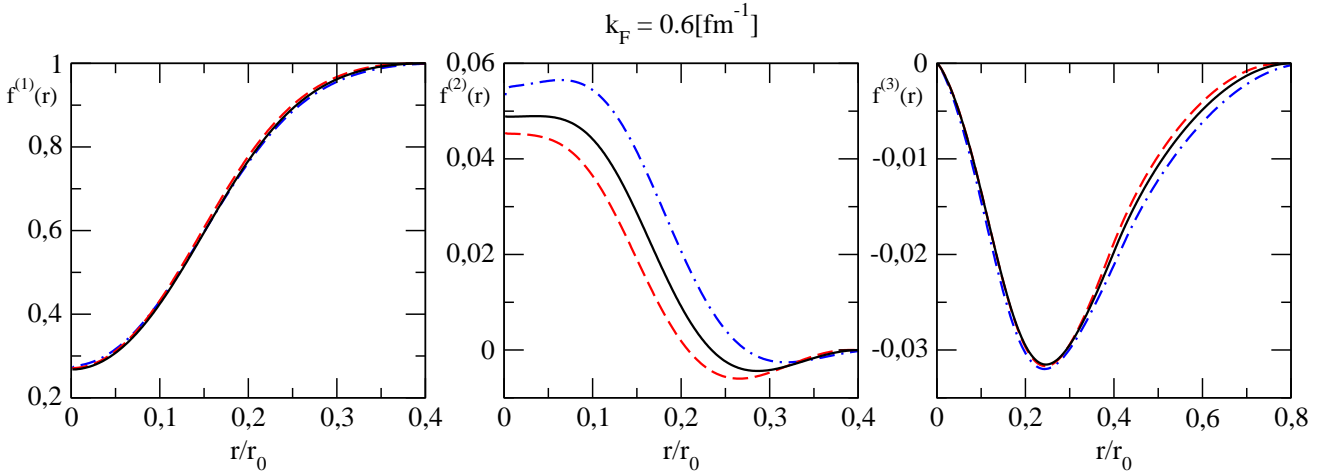


FIG. 2: (colored online) The central, spin and tensor correlation functions at the $k_F = 0.6 \text{ fm}^{-1}$ for the A8' potential. The dash-dotted, blue lines are the normal phase correlations. The dashed and solid, black lines are the BCS correlations without and with vertex corrections, correspondingly.

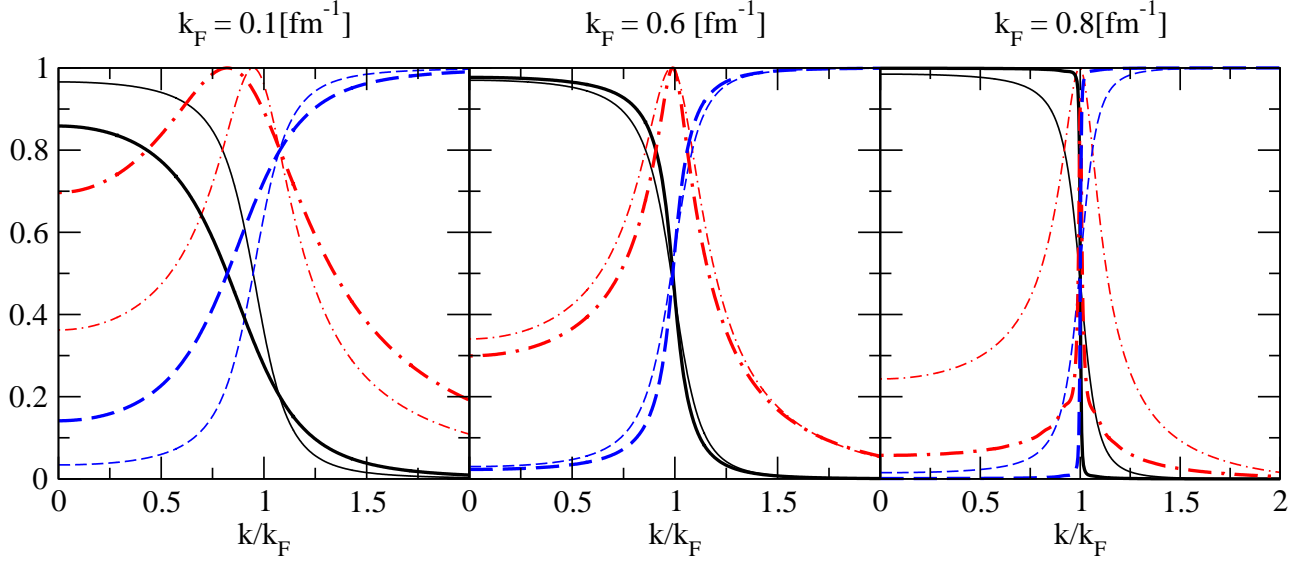


FIG. 3: (colored online) $v^2(k)$ (solid, black lines), $2v(k)u(k)$ (dash-dotted, red lines) and $u^2(k)$ (dashed, blue lines) amplitudes obtained from the A8' potential at three densities. The thin lines are the pure BCS results; the thick ones represent the correlated BCS amplitudes.

-
- [1] S. Fantoni, Nucl. Phys. **A363**, 381 (1981).
[2] A. B. Migdal, Sov. Phys. JETP **10**, 176 (1960), [Zh. Eksp. Theor. Fiz., **37**, 249 (1960)].
[3] S. Tsuruta, Phys. Rept. **292**, 1 (1998).
[4] H. Heiselberg and M. Hjorth-Jensen, Phys. Rept. **328**, 237 (2000), [nucl-th/9902033].
[5] J. A. Sauls, in *Cesme Lectures on "Timing Neutron Stars"*, NATO-ASI, Series C, April 1988, edited by H. Ögelman, E. P. J. van den Heuvel, and J. van Paradis (Kluwer Academic Press, 1989), vol. 262, pp. 441–490.
[6] M. A. Alpar and D. Pines, in *Proc. The Los Alamos Workshop "Isolated Pulsars"*, edited by K. A. Van Riper, R. Epstein, and C. Ho (Cambridge University Press, 1993).
[7] N. Bohr, B. R. Mottelson, and D. Pines, Phys. Rev. **110**, 936 (1958).
[8] L. N. Cooper, R. L. Mills, and A. M. Sessler, Phys. Rev. **114**, 1377 (1959).
[9] J. Bardeen, L. N. Cooper, and J. R. Schrieffer, Phys. Rev. **108**, 1175 (1957).
[10] E. Feenberg, in *Theory of Quantum Fluids* (Academic Press, 1969).
[11] M. Baldo, in *Nuclear Methods and the Nuclear Equation of State*, edited by M. Baldo (World Scientific, 1999).
[12] A. Vonderfecht, W. Dickhoff, and A. Polls, Nucl. Phys. **A555**, 1 (1993).
[13] R. B. Wiringa, S. C. Pieper, J. Carlson, and V. R. Pandharipande, Phys. Rev. **C62**, 044310 (2000).
[14] R. B. Wiringa, F. Ficks, and A. Fabrocini, Phys. Rev. **C38**, 1010 (1988).
[15] A. Fabrocini, F. Arias de Saavedra, and G. Co', Phys. Rev. **C61**, 044302 (2000).
[16] J. M. C. Chen, J. W. Clark, E. Krotscheck, and R. A. Smith, Nucl. Phys. **A451**, 509 (1986).
[17] J. M. C. Chen, J. W. Clark, R. D. Davé, and V. V. Khodel, Nucl. Phys. **A555**, 59 (1993).
[18] R. V. J. Reid, Ann. of Phys. **50**, 411 (1968).
[19] V. R. Pandharipande and R. B. Wiringa, Rev. Mod. Phys. **51**, 821 (1979).
[20] S. Fantoni and S. Rosati, Nuovo Cim. **A25**, 593 (1975).
[21] M. A. Alpar, W. Brinkmann, Ü. Kizilogo, H. Ögelman, and D. Pines, Astron. Astrophys. **229**, 133 (1990).
[22] S. Fantoni and V. R. Pandharipande, Nucl. Phys. **A427**, 473 (1984).
[23] A. Sarsa, S. Fantoni, K. E. Schmidt, and F. Pederiva, Phys. Rev. **C68**, 024308 (2003).
[24] J. Carlson, S.-Y. Chang, V. R. Pandharipande, and K. E. Schmidt, Phys. Rev. Lett. **91**, 050401 (2003).
[25] A. Fabrocini, S. Fantoni, A. Y. Illarionov, and K. E. Schmidt, Phys. Rev. Lett. **95**, 192501 (2005).
[26] I. E. Lagaris and V. R. Pandharipande, Nucl. Phys. **A359**, 331 (1981).
[27] A. Akmal, V. R. Pandharipande, and D. G. Ravenhall, Phys. Rev. **C58**, 1804 (1998), nucl-th/9804027.
[28] A. Fantoni and A. Fabrocini, Lecture Notes in Phys. **Vol. 510**, 119 (1998).
[29] A. J. Leggett, Rev. Mod. Phys. **47**, 331 (1975), [Erratum: Rev. Mod. Phys. **48**, 357 (1976)].
[30] V. A. Khodel, V. V. Khodel, and J. W. Clark, Nucl. Phys. **A598**, 390 (1996).
[31] R. C. Kennedy, Nucl. Phys. **A118**, 189 (1968).

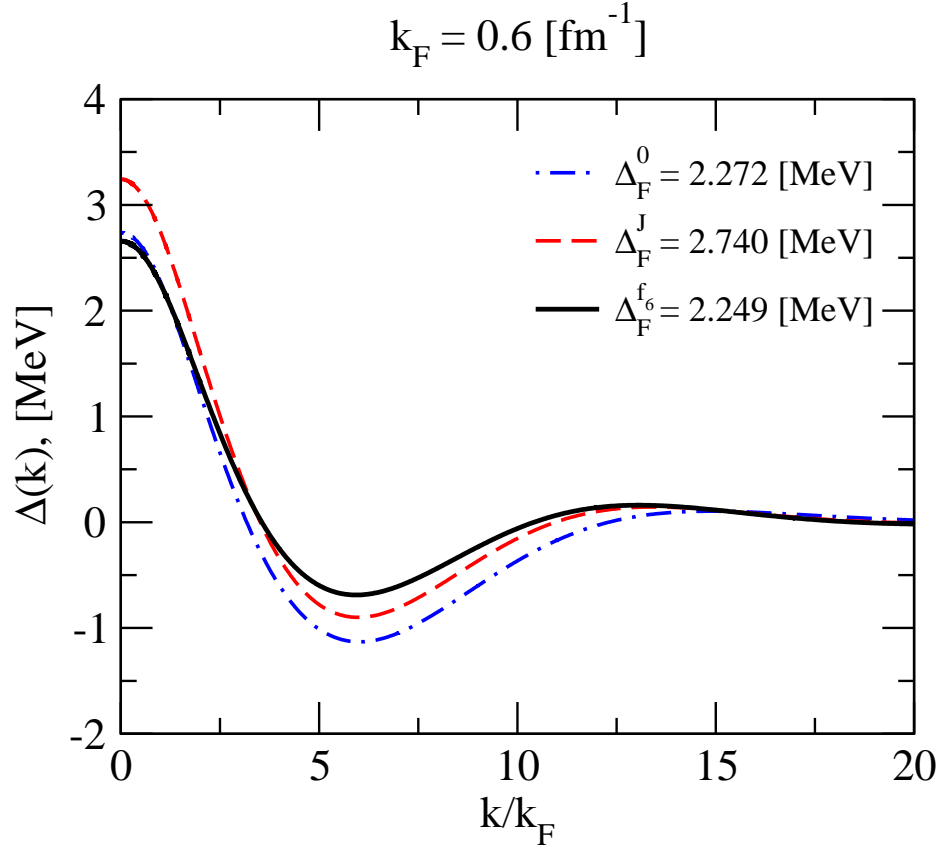


FIG. 4: (colored online) $\Delta(k)$, in MeV, obtained for the A8' model at $k_F = 0.6 \text{ fm}^{-1}$. The dash-dotted, blue line is the pure BCS solution; the dashed, red line represents the Jastrow correlates BCS case; the solid, black line is the fully correlated BCS solution.

[32] U. Lombardo and H.-J. Schulze, in *Physics of neutron Stars Interior*, edited by D. Blaschke, N. K. Glendenning, and A. Sedrakian (Springer (Berlin), 2001), vol. 578, p. 30.

[33] L. G. Cao, U. Lombardo, and P. Schuck, *Phys. Rev. C* **74**, 064301 (2006).

[34] S. Fantoni, A. Y. Illarionov, and K. E. Schmidt, in preparation (2007).

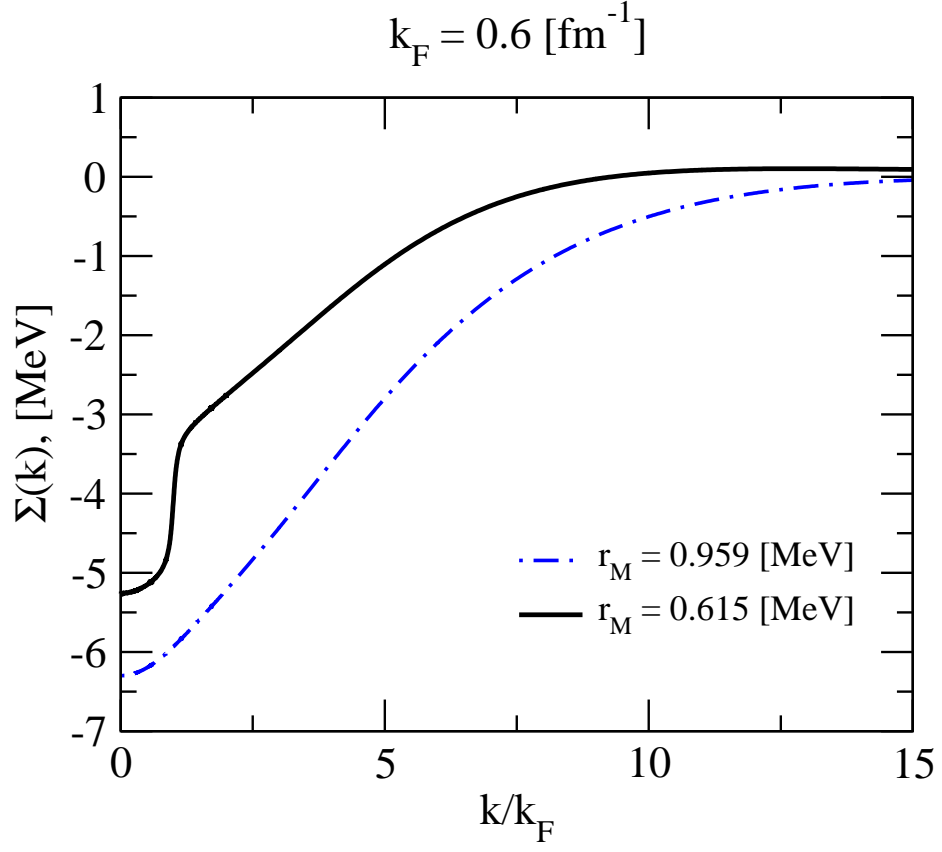


FIG. 5: (colored online) The self-energy $\Sigma(k)$, in MeV, for the BCS (dash-dotted, blue line) and correlated BCS (solid, black line) cases for the A8' model at $k_F = 0.6 \text{ fm}^{-1}$.

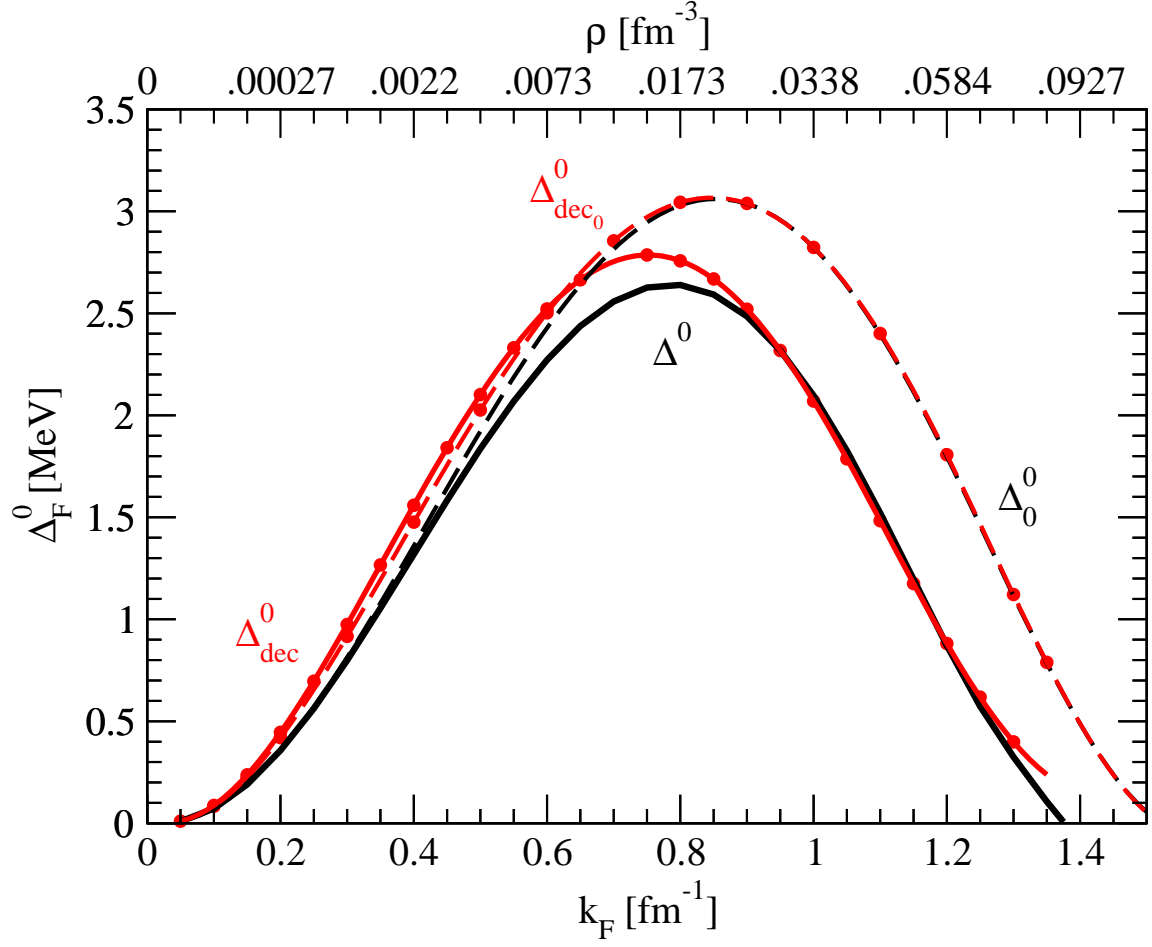


FIG. 6: 1S_0 pairing gaps obtained from the $A\delta'$ potential in the uncorrelated BCS case. The curves labeled $\Delta_{\text{dec}_0}^0$ and Δ_{dec}^0 are calculated in the decoupling approximation, without and with self-energy insertions, respectively. The remaining curves refer to the full solution (Δ_0^0 with $\Sigma(k) = 0$ and Δ^0 with $\Sigma(k) \neq 0$).

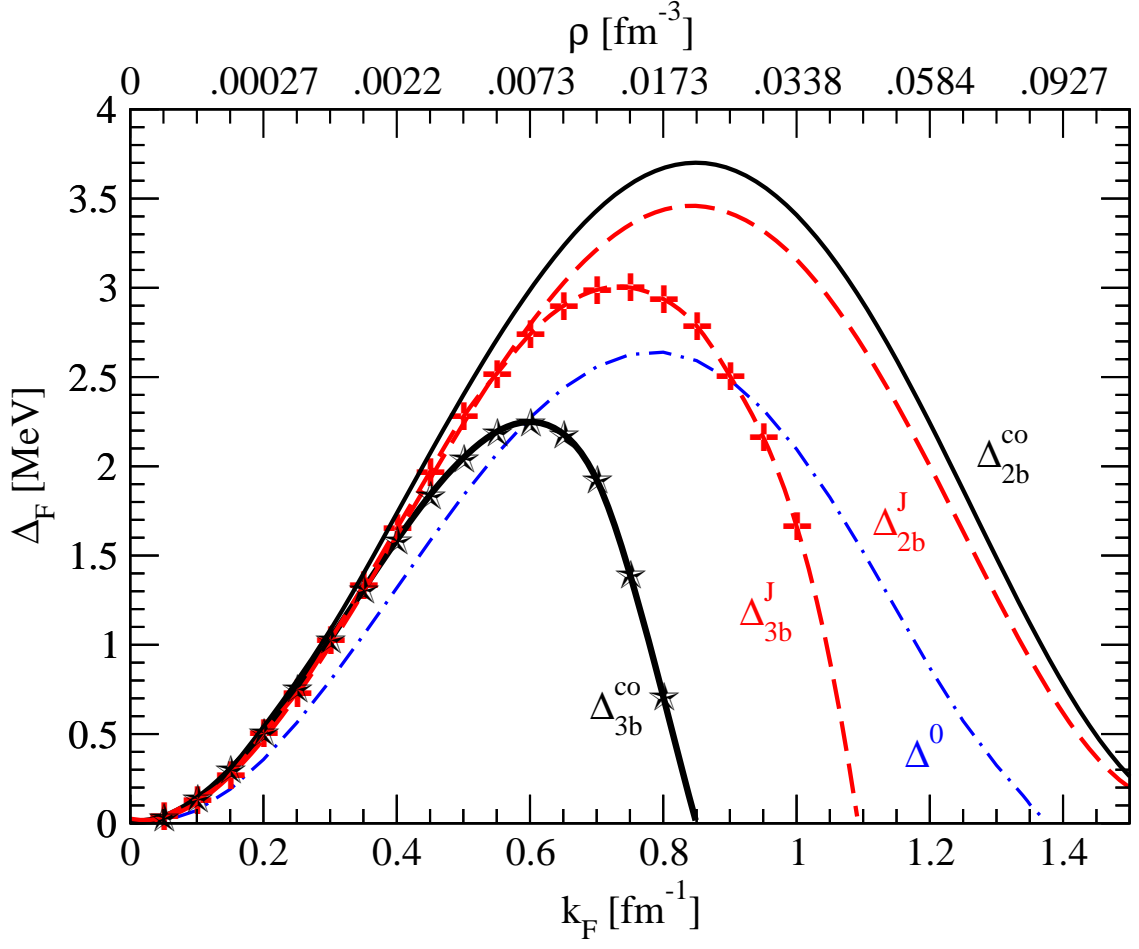


FIG. 7: $A8' \ ^1S_0$ pairing gaps for different correlations and levels of the cluster expansions. See text.

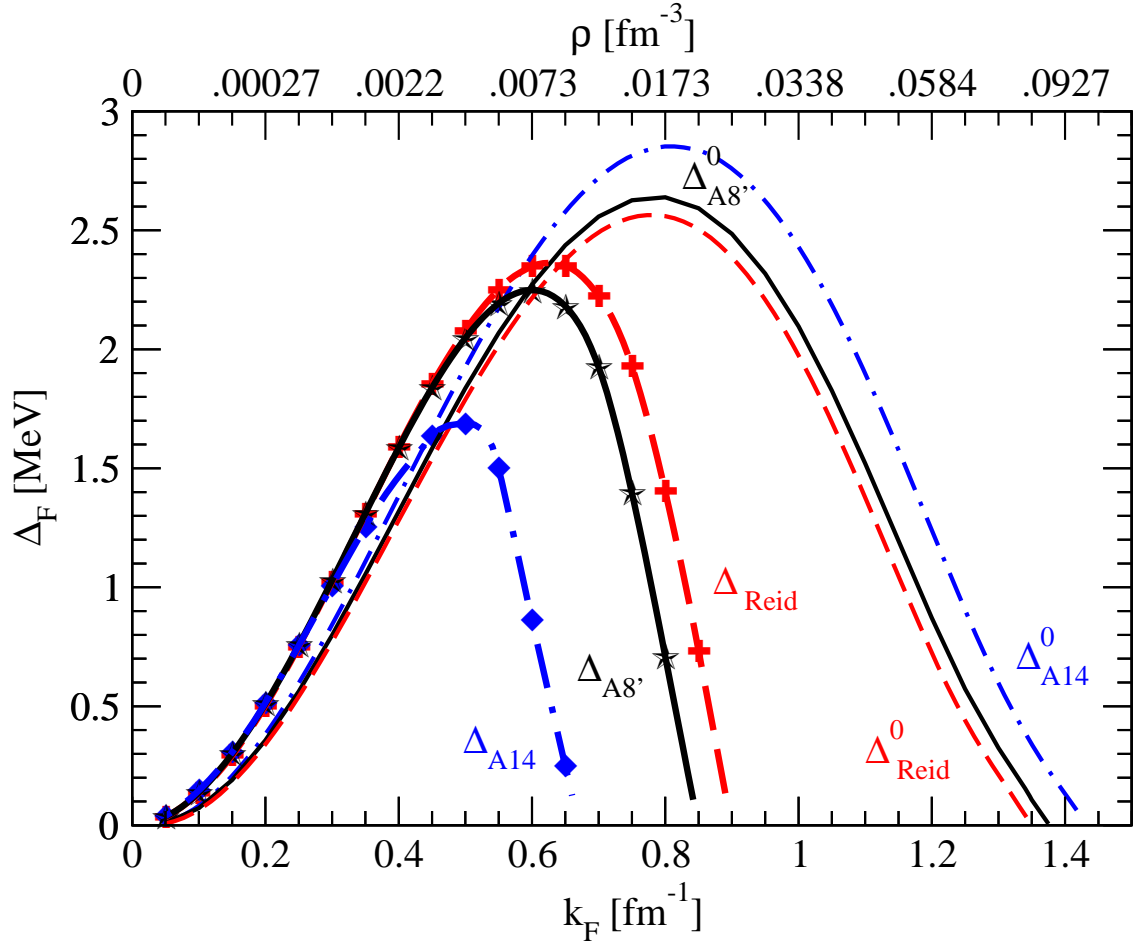


FIG. 8: 1S_0 pairing gaps for different nucleon-nucleon potentials.